

REPORT DOCUMENTATION PAGE

Form Approved
OMB No. 0704-0188

Public reporting burden for this collection of information is estimated to average 1 hour per response, including the time for reviewing instructions, searching existing data sources, gathering and maintaining the data needed, and completing and reviewing the collection of information. Send comments regarding this burden estimate or any other aspect of this collection of information, including suggestions for reducing this burden, to Washington Headquarters Services, Directorate for Information Operations and Reports, 1215 Jefferson Davis Highway, Suite 1204, Arlington, VA 22202-4302, and to the Office of Management and Budget, Paperwork Reduction Project (0704-0188), Washington, DC 20503.

1. AGENCY USE ONLY (Leave Blank)	2. REPORT DATE 25 Sep 99	3. REPORT TYPE AND DATES COVERED Final Technical Report 26 Sep 97 - 25 Sep 99	
4. TITLE AND SUBTITLE Manufacturable IR Photonic Crystals Based on Interferometric Lithography		5. FUNDING NUMBERS DAAG55-97-1-0373	
6. AUTHORS Brueck, S.R.J. Malloy, K.J.			
7. PERFORMING ORGANIZATION NAME(S) AND ADDRESS(ES) The University of New Mexico Center for High Technology Materials 1313 Goddard SE Albuquerque, NM 87106		8. PERFORMING ORGANIZATION REPORT NUMBER 3-49671FTR	
9. SPONSORING / MONITORING AGENCY NAME(S) AND ADDRESS(ES) U.S. Army Research Office P.O. Box 12211 Research Triangle Park, NC 27709-2211		10. SPONSORING / MONITORING AGENCY REPORT NUMBER ARO 37662.1-PH	
11. SUPPLEMENTARY NOTES The views, opinions and/or findings contained in this report are those of the authro(s) and should not be construed as an official Department of the Army position, policy or decision, unless so designated by other documentation.			
12a. DISTRIBUTION / AVAILABILITY STATEMENT Approved for public release, distribution unlimited		12b. DISTRIBUTION CODE	
13. ABSTRACT (Maximum 200 words) Periodic structures were designed, fabricated and characterized to control the emission of electromagnetic radiation. These electromagnetic crystals were fabricated using interferometric lithography, a technique that lends itself to large area periodic structures. The characterization was done using a Fourier Transform Infra-red Spectrometer. Extensive rigorous modeling was developed based on reigorous coupled-wave analysis and was shown to provide a route to "design-to-performace" for these structures.			
14. SUBJECT TERMS Photonics, Infrared photonic crystals, interferometric lithography		15. NUMBER OF PAGES 14	
		16. PRICE CODE NSP	
17. SECURITY CLASSIFICATION OF REPORT UNCLASSIFIED	18. SECURITY CLASSIFICATION OF THIS PAGE UNCLASSIFIED	19. SECURITY CLASSIFICATION OF ABSTRACT UNCLASSIFIED	20. LIMITATION OF ABSTRACT UNL

20010222 057

Final Report – 09/25/99
HIDE

Abstract

Periodic structures were designed, fabricated and characterized to control the emission of electromagnetic radiation. These electromagnetic crystals were fabricated using interferometric lithography, a technique that lends itself to large area periodic structures. The characterization was done using a Fourier Transform Infra-red Spectrometer. Extensive rigorous modeling was developed based on rigorous coupled-wave analysis and was shown to provide a route to “design-to-performance” for these structures.

Electromagnetic crystals are periodic structures that can be used to control the emission of electromagnetic radiation. The goal of the HIDE program is to directly control the emissivity of an object. The fabrication of the crystals is based on interferometric lithography (see attachment for a description of this method). This is a technique whereby two laser beams are interfered to establish a periodic pattern on a sample. Using standard lithography techniques, the pattern is transferred to the chosen material system. Currently, the material system of choice is silicon on sapphire and bulk silicon. In these material systems, we are able to etch a periodic pattern of air holes in the silicon sample. In addition, the material system can be metallized to obtain higher responsivity in a smaller area. Keep in mind that the system being tested is simply a two-dimensional electromagnetic crystal that is finite in the third dimension. Remarkably, the need for a three-dimensional structure to achieve the desired result is not apparent. We have independently shown that omni-directional stop bands can be achieved using simply a one-dimensional stack of alternating dielectric material. Although a “cute” solution, the utility of such a solution remains to be seen. We have focused mainly on a two-dimensional system.

One of the main goals in the program was to “build to design.” The design is done using rigorous coupled wave analysis (RCWA). The mathematical formulation can be found in the attached paper. The code has been verified based on various published results for slightly metallic and dielectric structures. The structures that are being modeled are shown in the figures below. Extending the technique to highly metallic structures produced a convergence problem. Although qualitative results can be achieved with RCWA, quantitatively the results did not agree with the experiment. The experiment was performed using a Fourier Transform Infra-red Spectrometer (FTIR).

Using RCWA as a design tool, a variety of structures were fabricated, characterized and modeled. Figures 1-3 indicate a small subset of the data obtained. The limitations in the model become apparent as the structure periodicity and aspect ratio are varied. Figures 1, 2 and 3 shows the comparison of the experimental data with the results of the RCWA for

a periodicity of 1.5 micron, 1.6 micron and 1.7 micron, respectively. The fill factor in all cases was 40%. There is a dip in the transmission response in both the calculation and the experimentally obtained results. This dip is due to the interference of the waves as they pass through the sample. By changing the periodicity, the location in frequency of the dip can be controlled as shown in the comparison between Figure 1 and Figure 2. Keep in mind that the computations were done *prior* to the fabrication of the samples, thus indicating our ability to build to design. Qualitatively, the agreement is very good for Figure 1. As the periodicity of the structure is increased, there is an issue with the convergence of the code. Quantitatively there is substantial discrepancy. The discrepancy can be attributed to two issues. The first is that in the experiment the back surface of the wafer is unpolished. This leads to a substantial scattering loss in transmission due to the rough surface on the back of the wafer. The scattering loss reduces the amount of energy that impinges on the detector, thus indicating a lower transmission response. In addition, the model assumes an infinite substrate, which will further increase this discrepancy. The second issue is the convergence of the code. The technique that is currently being implemented uses a Fourier basis to expand the fields in the periodic structure. For metallic structures that have square symmetry (square "holes" in a square pattern), a few terms in the Fourier basis are sufficient to produce accurate results. In our system, we employ circular symmetry due to the ease of fabrication. In the case of circular symmetry, a stair-step approximation is necessary for the atoms. This stair-step requires an unrealistic number of plane waves to converge. The circular symmetry requires an alternative basis to efficiently expand the fields that we are currently investigating. Thus we observe a discrepancy between calculations and experimental results. Note that as the periodicity is increased, the discrepancy between experiment and computation increases. This is again due to the lack of convergence in our method.

One of the main focuses of our effort has been to determine the angular dependence of the sample. Figure 4 shows the experimental result of the azimuthal dependence of the sample in reflection. Note that there is symmetry in the response reflects the triangular symmetry of the sample. The symmetry is indicated in the bright spots that exist at a wavelength of $6\mu\text{m}$. There are bright spots, which correspond to approximately 50% reflectivity at angles of approximately 45° , 105° , 165° , 225° , 285° , and 345° . The angles are determined by the orientation of the sample on the measurement set-up. Note that the angles of high reflectivity are separated by approximately 60° . Consider the wavelengths between $2\mu\text{m}$ and $3\mu\text{m}$. The reflectivity of the sample changes between 40% and 65% as a function of angle. This is an extremely desirable property. The reflectivity varies as a function of azimuthal angle. Currently we are investigating controlling the variation of the reflectivity as a function of the azimuthal angle.

Azimuthal Reflectivity, 30° incidence

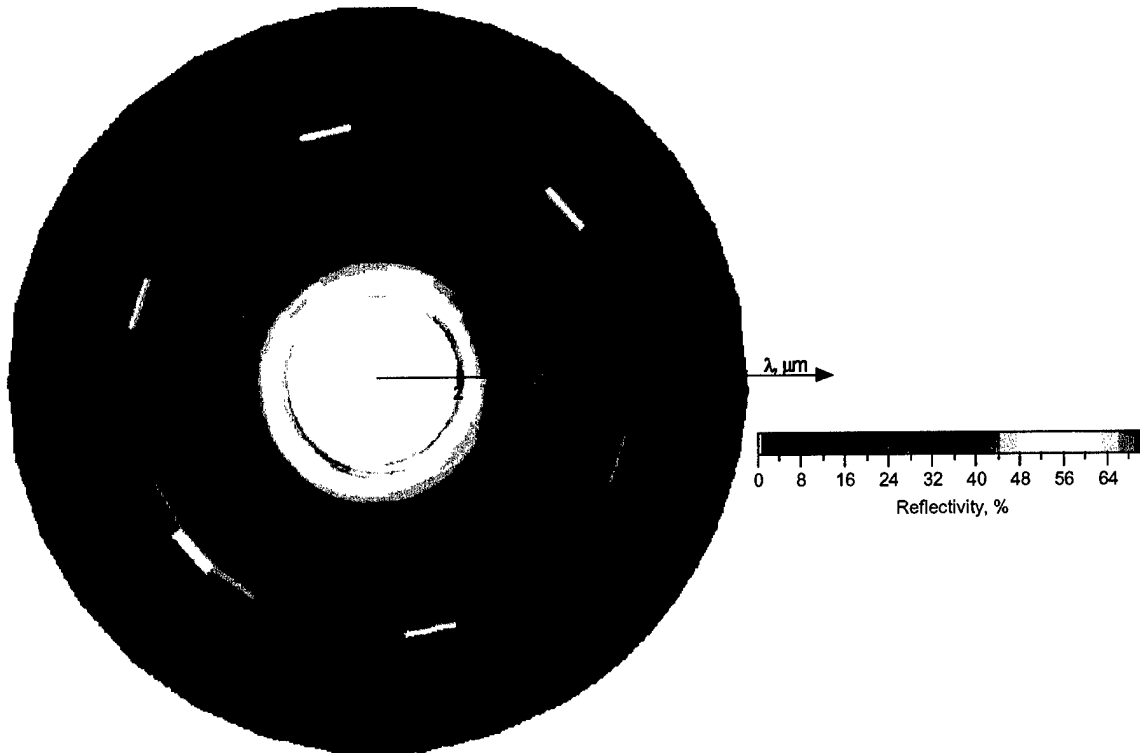


Figure 4. Reflectivity of the sample as a function of azimuthal angle and wavelength at an incident angle of 30°. The response reflects the triangular symmetry of the sample.

We have investigated methods of improving the convergence of our computational technique, including paralleling the code to increase the number of plane waves that the computation can handle and identifying various basis functions that will more efficiently reflect the symmetry of the structure. Fabrication efforts involve investigating multi-layer techniques to implement in conjunction with the interferometric lithography. These efforts remain the subject of other ongoing investigations.

Gold dots on Silicon
pitch = 1.5 microns, diameter = 0.6 microns
height = 0.1 microns

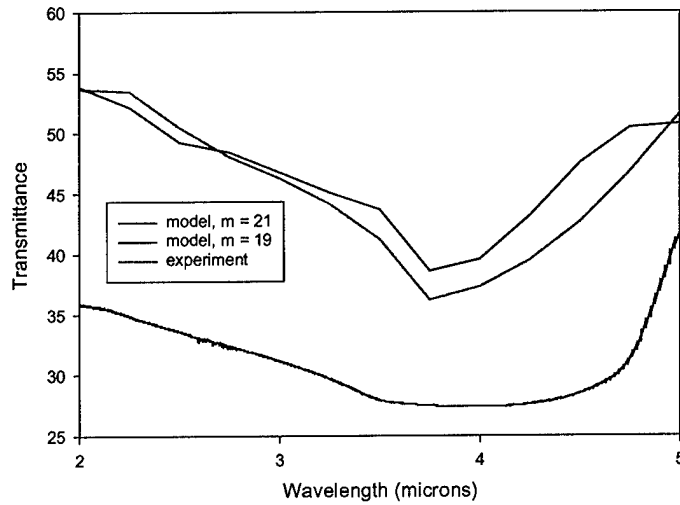
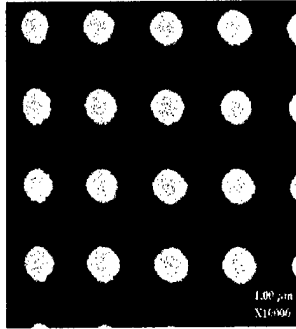


Figure 1. Gold dots on Silicon. The pitch is designed to 1.5 microns and the diameter of the holes is 0.6 microns. The height of the two-dimensional pattern is 0.1 microns. The SEM picture is shown on the left. For the figure on the right, the lower curve is the experimental result and the upper curves are the calculations for a variation in the number of plane waves in the expansion.

Gold dots on Silicon
pitch = 1.6 microns, diameter = 0.64 microns
height = 0.1 microns

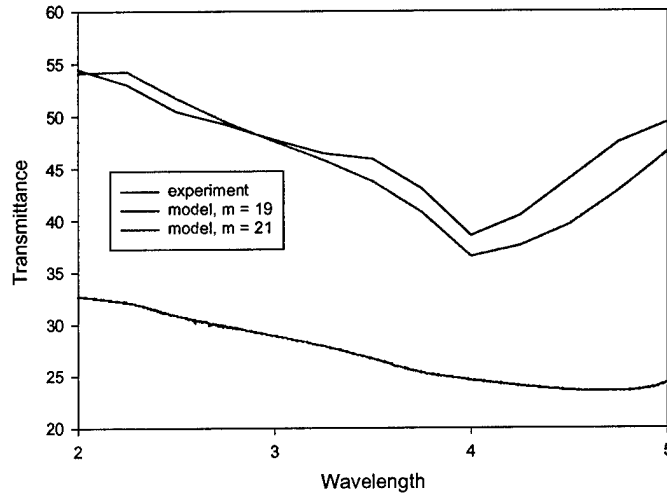
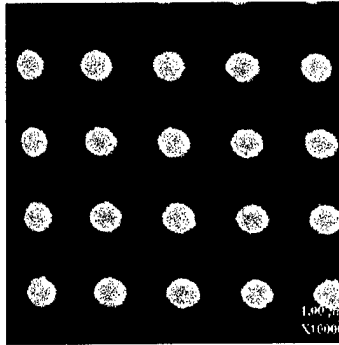


Figure 2. Gold dots on Silicon. The pitch is designed to 1.6 microns and the diameter of the holes is 0.64 microns. The height of the two-dimensional pattern is 0.1 microns. The SEM picture is shown on the left. For the figure on the right, the lower curve is the experimental result and the upper curves are the calculations for a variation in the number of plane waves in the expansion.

Gold dots on Silicon
pitch = 1.7 microns, diameter = 0.68 microns,
height = 0.1 microns

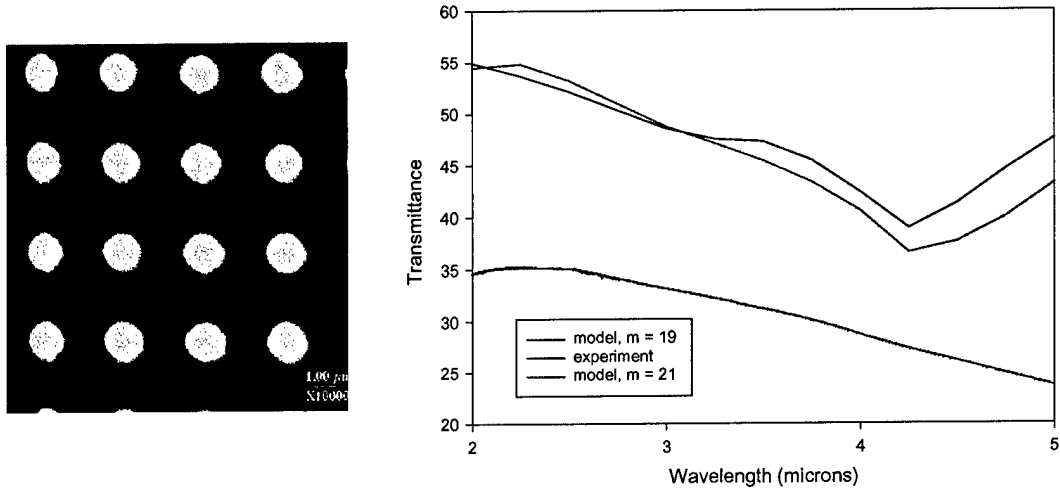


Figure 3 Gold dots on Silicon. The pitch is designed to 1.7 microns and the diameter of the holes is 0.68 microns. The height of the two-dimensional pattern is 0.1 microns. The SEM picture is shown on the left. For the figure on the right, the lower curve is the experimental result and the upper curves are the calculations for a variation in the number of plane waves in the expansion.

Metallic inductive and capacitive grids: Theory and Experiment

B. K. Minhas, W. Fan, K. Agi, S. R. J. Brueck and K. J. Malloy
Center for High Technology Materials, University of New Mexico
Albuquerque, New Mexico 87131

ABSTRACT

We present experimental validation of theoretical modeling of metallic crossed gratings for the mid infrared (2-5 μm) regime. The gratings are fabricated using interferometric lithography and modeled using a rigorous coupled wave analysis. The electromagnetic properties of these gratings are explained in terms of surface plasmon excitation, which couples the incident light into the inhomogeneous modes of the gratings.

I. Introduction

Crossed gratings (of which metallic grids are special cases) find numerous applications in the entire electromagnetic spectrum. They are used in the microwave regime as filters and for making efficient antennas¹. In the far infrared, they find applications as polarizers, beam splitters and mirrors². Their use as filters^{3,4} and solar selective surfaces⁵ in the visible and near infrared regime has also been demonstrated. Recently there has been interest in the behavior of subwavelength metallic crossed gratings^{6,7} (inductive grids in particular) with potential applications for novel optoelectronic devices. In that work, the properties of metallic inductive grids were attributed to surface plasmon excitation. Although this model explains the wavelength position of the experimental features, a rigorous diffraction model is necessary to both accurately describe all experimental features and as a tool for crossed gratings design.

In this paper we present a rigorous diffraction model validated by experimental data for inductive as well as capacitive subwavelength metallic crossed gratings under normal plane wave illumination. We present the effects of variation of grating parameters on the mid-IR transmission spectrum. To the best of our knowledge, this is the first rigorous numerical modeling and experimental verification of metallic inductive and capacitive grids.

In the remaining part of this letter, we briefly explain the fabrication and experimental characterization of crossed gratings. This is followed by the convergence behavior of the numerical model; comparison of the surface plasmons model with the rigorous diffraction model and finally the experimental verification of the diffraction model.

II. Fabrication and experimental characterization

The grating used to validate the modeling were fabricated using interferometric lithography and lift-off pattern transfer. A double polished silicon sample is used as a substrate material, as it is transparent in the ($2\mu\text{m} - 5\mu\text{m}$) regime. After coating the substrate with photoresist, interferometric lithography⁸ is used to expose the pattern. This is followed by developing the photoresist and metallization by e-beam evaporation of gold. The final step is an acetone jet lift-off leaving the desired pattern.

Experimental characterization of these structures is done using Fourier transform infrared spectroscopy (FTIR), and all the results presented in this paper are for normal incidence transmission in the mid-infrared ($2 - 5\mu\text{m}$) range.

III. Modeling

Numerical modeling of metallic crossed gratings is a computationally intensive problem. Previously, crossed gratings were modeled in the microwave regime by assuming the metallic scatterers to have infinite conductivity⁹⁻¹¹. While this approximation works well at microwave frequencies where metals have very high conductivity, its use but for the visible and ultraviolet is clearly inappropriate. In the infrared, the suitability of the infinite conductivity approximation is uncertain. We use a rigorous diffraction model to avoid these questions at the cost of higher computational complexities.

Since the late 1970s, significant work has been done in modeling crossed gratings with finite conductivity. Derrick^{12,13}, Harris¹⁴ proposed a model based on the co-ordinate transformation, Vincent¹⁵ used a finite difference method and Bruno¹⁶ employed a variation of boundaries method. More recently, Kettunen et al.,¹⁷ presented numerical results for metallic inductive grids based on the rigorous coupled wave analysis (RCWA)¹⁸. Their modeling was done principally for the case of rectangular scatterers and included the dielectric expansion changes suggested by Li¹⁹ to improve the convergence of the algorithm. Here, we present modeling for finite conductivity, circular, metallic scatterers arranged in a square lattice on a silicon substrate. Results for both capacitive and inductive grids are described.

III.a Convergence of the numerical model

Our model is based on RCWA and incorporates the modifications suggested by Li¹⁹. While these modifications work well for rectangular scatterers, in our case, the convergence of the algorithm slows when the scatterers are circular metallic patches. We therefore restrict the computations to normal plane wave illumination and take advantage of the symmetry of the configuration²⁰ to reduce the numerical size of the problem. Specifically for normal incidence, the equivalence of the positive and negative Fourier coefficients allows reduction of the final eigenvalue problem from $(2N+1)^2$ to $(N+1)^2$,

where N is the number of spatial harmonics for both the dielectric expansion and the field expansion. This allows us to study the behavior of the solution for reasonably high values of N for an algorithm implemented on a personal computer.

Validating the performance of any numerical algorithm is an essential part of establishing the utility of the algorithm. Unlike the situation for one-dimensional gratings where the convergence properties of RCWA for metallic gratings are well-established [REFS], little is known of the behavior of two-dimensional RCWA algorithms. Initially, we examined the numerically calculated diffraction efficiency as a function of the mode number N up to the maximum number of modes as allowed by the computational resources. For the subwavelength grating of interest here, the diffraction efficiency is the ratio of the power in the 0th transmitted order to the incident power. Figure 1 shows the convergence behavior of the algorithm for a capacitive structure on silicon with the parameters detailed in the caption. From the figure, it may be seen that although the algorithm is well behaved its rate of convergence is slow. Nonetheless the variation in diffraction efficiency as a function of mode number N is at the most $\pm 5\%$ after $N = 15$. In the results

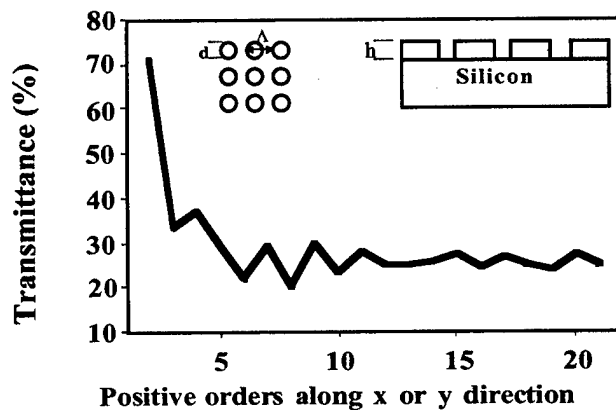


Figure 1: Convergence behavior of the model, $\Lambda = 1.20\mu\text{m}$, $d = 0.56\mu\text{m}$, $h = 0.1\mu\text{m}$, $\lambda = 4.0\mu\text{m}$, larger fonts, clearer lines, points, more accurately aligned drawings

shown in this paper we have used $N = 15$ for circular scatterers and assume the convergence error to behave similarly for all structures. However, the final proof of the validity of the two-dimensional RCWA lies in experimental verification. The remainder of our discussion details the agreement between the RCWA algorithm and experimental characterization of actual metallic crossed gratings.

III.b Previous work and the surface plasmon model

Previous experimental investigations of metallic sub-wavelength crossed grating in the infrared have described their behavior in terms of coupling into surface plasmons^{6,21}. In this model, momentum conservation is used to derive a simple design equation⁶ for the

condition necessary for normally incident radiation to couple into the inhomogeneous modes of the gratings. This condition is

$$\lambda/\Lambda = \{\epsilon_m \epsilon_d / [(i^2 + j^2)(\epsilon_m + \epsilon_d)]\}^{1/2}$$

here λ is wavelength of incident light, Λ is the pitch of the grating, i and j are integers and ϵ_m and ϵ_d are the real part of the permittivities of the metal and dielectric respectively.

The above equation can be used to excite surface plasmons at a given wavelength. To illustrate consider the case of metal-substrate coupling for incident wavelength of $\lambda = 4\mu\text{m}$, this gives a grating pitch of $\Lambda = 1.15\mu\text{m}$ for coupling light into the $(\pm 0, \pm 1)$ degenerate orders of the gratings. We verify this result using RCWA, as shown in the Fig. 2, for the case of inductive as well as capacitive grids. Here in order to save computational efforts we are using square scatterer instead of the circular scatterer, as the momentum conservation of the problem does not depend on the shape of the scatterer. As may be seen from figure, the surface plasmons calculations match very well with the rigorous diffraction model. We also note launching of several other inhomogeneous modes corresponding to different grating orders as well as air-metal surface plasmons coupling.

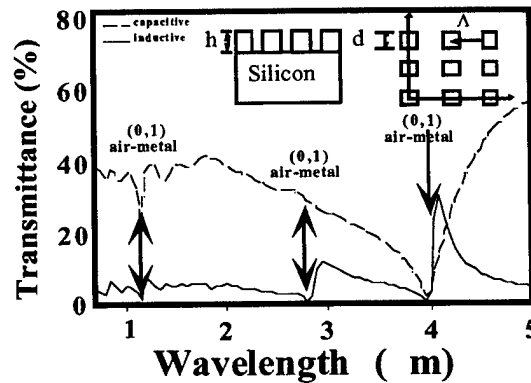


Figure 2: Surface plasmons coupling for the inductive and capacitive grids, fill factor = $0.5\mu\text{m}$, $h = 0.1\mu\text{m}$, $N = 10$ (a) inductive grids (b) capacitive grids

III.c Capacitive and inductive grids

From figure 2, we observe attenuation of incident radiation in case of capacitive grids and enhancement of radiation for the inductive grids. We experimentally verify this complementary behavior by fabricating inductive grids and capacitive grids of same pitch and height. This is shown in figures 3 and 4 along with the numerical computations. From the figures it may be noted that a very good match is obtained between rigorous diffraction model and experiment; furthermore, we observe strong excitation of surface

plasmons modes for the inductive grids, as compared to the capacitive grids. This is the subject of further study.

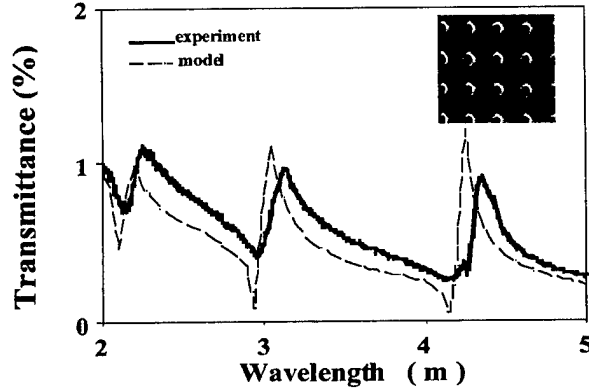


Figure 3: Inductive grid, air holes in gold on Si, $\Lambda = 1.20\mu\text{m}$, $d = 0.40\mu\text{m}$, $h = 0.1\mu\text{m}$

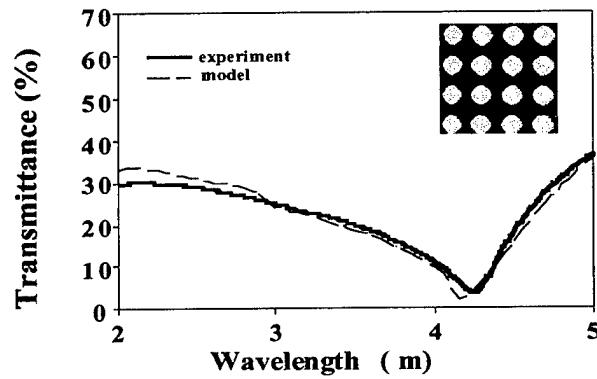


Figure 4: Capacitive grid, gold dots on Si, $\Lambda = 1.20\mu\text{m}$, $d = 0.76\mu\text{m}$, $h = 0.1\mu\text{m}$

III.d Fill factor study

Fill factor is defined as the fraction of the area of unit cell occupied by the scatterer; for circular scatterer this is simply given as $\pi/4(d/\Lambda)^2$. Surface plasmons coupling is a strong function of the grids fill factor. To verify this for capacitive grids we made samples of different fill factors by keeping the pitch and height of the periodic structures constant and varying only the diameter of the gold patches.

Figures 5 shows the experimental and numerical results for different fill factors. It may be noted that the model and experiment are much closer for higher fill factors, one reason for this may be that we are not taking into account the finite thickness of the substrate. Also from the figure we see that the surface plasmons coupling get stronger for higher fill factors and reaches a maximum value after a certain fill factor. We expect similar behavior for the case of inductive grids.

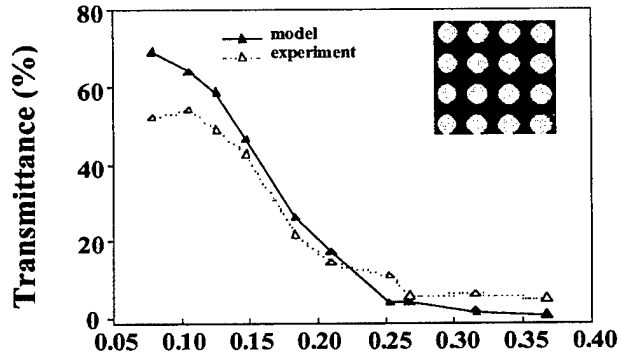


Figure 5: Fill factor variations, $\Lambda = 1.2\mu\text{m}$, $h = 0.1\mu\text{m} = 0.82\mu\text{m}$, $\lambda = 4.15\mu\text{m}$

IV. Conclusion

We have presented experimental and numerical results for metallic inductive and capacitive grids. A physical model based on surface plasmons coupling is used to study the behavior of these grids. This model is supplemented with a rigorous diffraction model to study effects of various grating parameters. Experimental and numerical evidence shows that the surface plasmons coupling is a strong function of the grids fill factor; it increases with bigger fill factor. We will present further details on the behavior of these grids in a future paper.

V. Acknowledgements

This research was supported by DARPA. One of the authors B. Minhas will like to thank Drs. Lifeng Li and Pasi Vahimaa for the help during the debugging stage of the diffraction code.

VI. References

- ¹T. K. Wu, Frequency Selective Surface and Grid Array, (John Wiley, 1995).
- ²R. Ulrich, Far-infrared properties of metallic mesh and its complementary structure, *Infrared Physics* **7**, 37-55 (1967).
- ³Song Peng and G. Michael Morris, Experimental demonstration of resonant anomalies in diffraction from two-dimensional gratings, *Optics Letters* **21** (8), 549-551 (1996).
- ⁴Song Peng and G. Michael Morris, Resonant scattering from two-dimensional gratings, *Journal of the Optical Society of America A* **13** (5), 993-1005 (1996).
- ⁵C. M. Horwitz, A new solar selective surface, *Optics Communications* **11** (2), 210-212 (1974).

- ⁶Tae Jin Kim and Tineke Thio and T. W. Ebbesen and D. E. Grupp and H. J. Lezec, Extraordinary optical transmission through subwavelength hole arrays, *Optics Letters* **24** (4), 256-258 (1999).
- ⁷T. W. Ebbesen and H. J. Lezec and H. F. Ghaemi and T. Thio and P. A. Wolff, Extraordinary optical transmission through subwavelength hole arrays, *Nature* **391**, 667-669 (1998).
- ⁸Xiaolan Chen and Saleem H. Zaidi and S. R. J. Brueck, Interferometric lithography of sub-micrometer sparse hole arrays for field-emission display applications, *Journal of Vacuum Science and Technology B* **14** (5), 3339-3349 (1996).
- ⁹Chao-Chun Chen, Transmission through a conducting screen perforated periodically with apertures, *IEEE transactions on Microwave Theory and Techniques* **18** (9), 627-632 (1970).
- ¹⁰Raj Mittra and Chi H. Chan and Tom Cwik, Techniques for Analyzing Frequency Selective Surfaces- a review, *Proceedings of IEEE* **76** (12), 1593-1615 (1988).
- ¹¹R. C. McPhedran and D. Maystre, On the theory and application of solar inductive grids, *Applied Physics* **14**, 1-20 (1977).
- ¹²G. H. Derrick and R. C. McPhedran and D. Maystre and M. Neviere, Crossed gratings: A theory and its applications, *Applied Physics* **18**, 39-52 (1979).
- ¹³R. Petit, *Electromagnetic Theory of Gratings*, (Springer-Verlag, 1980).
- ¹⁴T. W. Priest and J. B. Harris and J.R. Sambles and R. N. Thorpe and R. A. Watts, Optical response of bigratings, *Journal of the Optical Society of America A* **13** (10), 2041-2049 (1996).
- ¹⁵P. Vincent, A finite-difference method for dielectric and conducting crossed gratings, *Optics Communications* **26** (3), 293-296 (1978).
- ¹⁶O. P. Bruno and F. Reitich, Numerical solutions of diffraction problems: a method of variation of boundaries. iii. doubly periodic gratings, *Journal of the Optical Society of America A* **10** (5), 2551-2562 (1993).
- ¹⁷Ville Kettunen and Markku Kuittinen and Jari Turunen and Pasi Vahimaa, Spectral filtering with finitely conducting inductive grids, *Journal of the Optical Society of America A* **15** (10), 2783-2785 (1998).
- ¹⁸M. G. Moharam and Eric B. Grann and Drew A. Pommert and T. K. Gaylord, Formulation for stable and efficient implementation of the rigorous coupled wave analysis of binary gratings, *Journal of the Optical Society of America A* **12** (5), 1068-1076 (1995).
- ¹⁹Lifeng Li, New formulations of the Fourier modal method for crossed surface relief gratings, *Journal of the Optical Society of America A* **14** (10), 2758-2767 (1997).
- ²⁰Philippe Lalanne and Dominique Lemerrier-Lalanne, On the effective medium theory of subwavelength periodic structures, *Journal of Modern Optics* **43** (10), 2063-2085 (1996).
- ²¹H. Raether, *Surface Plasmons on smooth and rough surfaces and on gratings* (Springer-Verlag, 1988).